

Nernst Effect and Anomalous Transport in Cuprates: A Preformed-Pair Alternative to the Vortex Scenario

Shina Tan and K. Levin

James Franck Institute and Department of Physics, University of Chicago, Chicago, Illinois 60637

We address those puzzling experiments in underdoped high T_c superconductors which have been associated with normal state “vortices” and show these data can be understood as deriving from preformed pairs with onset temperature $T^* > T_c$. For uncorrelated bosons in small magnetic fields, and arbitrary T^*/T_c , we present the exact contribution to *all* transport coefficients. In the overdoped regime our results reduce to those of standard fluctuation theories ($T^* \approx T_c$). Semi-quantitative agreement with Nernst, ac conductivity and diamagnetic measurements is quite reasonable.

PACS numbers: 74.40.+k, 74.25.Fy, 74.72.-h

Keywords: high temperature superconductivity; superconducting fluctuation

Recent Nernst[1, 2] and ac conductivity[3] experiments have led to some of the most exotic indications for the normal state gap (or pseudogap) in the cuprates which, it is claimed, appear in the form of “vortices above T_c ”. More generally (but not universally) one associates the complex of pseudogap phenomena with some form of precursor superconductivity. While normal state vortices are most closely associated with the well known phase fluctuation scenario[4], a primary goal of this paper is to address these same anomalous transport data[2, 3] within the alternative pair fluctuation scheme[5, 6]. Pair fluctuations are non-condensed bosons which have as a natural antecedent the fluctuations of time dependent Ginsburg-Landau (TDGL) theory, and the associated description of their dynamics[7, 8, 9]. Bosonic degrees of freedom are additionally stabilized by going beyond the usual[7, 9] Gaussian approximation to TDGL. When their interactions are included at the self consistent Hartree level a fermionic pseudogap necessarily appears[10]: as a result of this depletion of the density of states, there are fewer fermions to which bosonic states can decay.

The anomalously short coherence length in the cuprates and the clear presence of a pseudogap has motivated a number of authors to extend this pair fluctuation approach to stronger than BCS attraction so that the bosonic degrees of freedom (and concomitantly, the fermionic pseudogap) appear at a temperature T^* which may be significantly larger than T_c . Below T_c the resulting superconducting state is mid-way between BCS and Bose Einstein condensation (BEC)[5, 11, 12]. Indeed, there is a close connection[13] between a pre-formed pair model belonging to a BCS-BEC crossover scheme[6] and a T-matrix based diagrammatic formulation of the Hartree-TDGL approach[10].

A second very important motivation for this work is to provide a natural extension of TDGL theory. The goal is to address higher temperatures T^* , well outside the usual limited range of applicability near T_c , where the bosonic field is described by classical fluctuation-dissipation[7, 8]. In the process we are able to compute exactly and compare with experiment, a wide variety of

transport coefficients. Such a mean field approach does not describe the order parameter fluctuations in the critical regime, so that critical exponents here belong to the Gaussian, rather than $3d - XY$ class. To proceed, we construct a simplified model of charged bosons subject to quantum dissipation, which has TDGL (with a non-BCS parameter set) as its special limit. Pair fluctuations involve the continuous dissociation and recombination of fermion pairs. To simulate this behavior we follow Caldeira and Leggett and treat the fermions as reservoir harmonic oscillators[14, 15] coupled to the bosons. Coulomb and hard core interactions between bosons are treated at the same level as in Hartree-approximated TDGL. While Coulombic effects are profound for order parameter fluctuations (below T_c and in the narrow critical regime above), here they are less important, for precisely the same reasons that they are omitted in traditional TDGL[7]. As in BCS theory, Coulomb interactions may also enter the binding and unbinding of pairs insofar as they renormalize or even, for non- s wave superconductors[16], stabilize the attraction between fermions.

To gain a deeper understanding of the essence of TDGL and of its prior success away from the pseudogap (or underdoped) regime[9], we thus study a Hamiltonian describing bosons in the presence of a fermionic reservoir

$$\begin{aligned}
 H = & \sum_{\mathbf{ux}} \varepsilon_{\mathbf{ux}} \psi_{\mathbf{x}}^\dagger(t) \exp(-iqC_{\mathbf{ux}}(t)) \psi_{\mathbf{x}+\mathbf{u}}(t) \\
 & + \sum_{\mathbf{x}} q\varphi \psi^\dagger \psi + \sum_{i\mathbf{x}} \left\{ (a_i + q\varphi) w_i^\dagger w_i + \eta_i \psi^\dagger w_i + \eta_i^* w_i^\dagger \psi \right\} \\
 & + \sum_{i\mathbf{x}} \left\{ (b_i - q\varphi) v_i^\dagger v_i + \zeta_i \psi^\dagger v_i^\dagger + \zeta_i^* v_i \psi \right\}. \quad (1)
 \end{aligned}$$

Here $\psi_{\mathbf{x}}(t)$ is the boson annihilation operator at lattice site \mathbf{x} and time t , (φ, \mathbf{A}) is the electromagnetic potential, $\hbar = \epsilon_0 = k_B = 1$ and $q = -2e$ is the boson charge. Annihilation operators for the reservoir, w_i and v_i (with coupling constants η_i and ζ_i), are associated with positive and negative frequencies respectively, although the energies a_i and b_i are both positive. $\varepsilon_{\mathbf{ux}}$ is the hopping

matrix element and $C_{\mathbf{ux}}(t) \equiv \int_0^1 ds u_a A_a(\mathbf{x} + s\mathbf{u}, t)$. Surface effects appear via the \mathbf{x} dependence of $\varepsilon_{\mathbf{0x}}$ which also contains the Hartree interaction between bosons.

The coupled equations of motion for the operators ψ , w_i and v_i may be reduced to a single equation for $\psi(\mathbf{x}, t)$ in the $\varphi(\mathbf{x}, t) = 0$ gauge, which depends, in turn, on a time integral from t_0 to t involving $\psi(\mathbf{x}, t')$. The reservoir fields $w_i(\mathbf{x}, t)$ and $v_i(\mathbf{x}, t)$ enter only in terms of their values at initial time t_0 . We take the coupling η_i and ζ_i between ψ and each reservoir field to be infinitesimal[14], so that the reservoir obeys ideal Bose statistics. The resultant self energy in the boson propagator is found to be

$$\widetilde{\Sigma}_2(\omega) \equiv 2\pi \sum_i |\eta_i|^2 \delta(\omega - a_i) - 2\pi \sum_i |\zeta_i|^2 \delta(\omega + b_i). \quad (2)$$

where, $\widetilde{\Sigma}_2(\omega)$ is smooth while approaching zero as $\omega \rightarrow \pm\infty$.

In the zero-field case, the density of the bosons is $\frac{1}{V} \langle \psi^\dagger \psi \rangle = \int \frac{d^d k}{(2\pi)^d} \frac{d\omega}{2\pi} \widetilde{A}(\mathbf{k}\omega) b(\omega)$, where $b(\omega) \equiv 1/(\exp(\omega/T) - 1)$ and V is the volume associated with each lattice site and $\widetilde{A}(\mathbf{k}\omega) = \text{Re} 2i\widetilde{T}(\mathbf{k}\omega)$ with boson propagator or ‘‘T-matrix’’ given by

$$\widetilde{T}(\mathbf{k}\omega) \equiv \left(\omega - \widetilde{\Sigma}_1(\omega) - \varepsilon(\mathbf{k}) + \frac{i}{2} \widetilde{\Sigma}_2(\omega) \right)^{-1}. \quad (3)$$

Here $\varepsilon(\mathbf{k}) \equiv \sum_{\mathbf{u}} \varepsilon_{\mathbf{u}} \exp(ik_a u_a)$ is the boson dispersion, and $\widetilde{\Sigma}_1(\omega) \equiv P \int \frac{d\omega'}{2\pi} \frac{1}{\omega - \omega'} \widetilde{\Sigma}_2(\omega')$. $\widetilde{\Sigma}_2(\omega)$ depends only on ω for our localized reservoir fermions. This simplification is supported principally by the fact that Eq. (3) captures the key physics found in microscopic schemes[5, 17], where it is sufficient to consider just the leading order \mathbf{k} dependences. Differences between this previous strong coupling T-matrix approach[5, 17] and the present phenomenological boson model, are to be associated with fine ω structure from the fermionic pseudogap[17], as well as different high ω asymptotics. The ensuing simplification of transport calculations, however, makes our boson model far more useful.

As expected for a reservoir, the parameters a_i , b_i , η_i and ζ_i are not readily characterized nor are they particularly fundamental. The essence of the present approach is to establish that one can characterize the transport of bosons without knowing the details of the reservoir, but simply using generic features of microscopic T-matrix theory[5, 13, 17] and its relation to the Hartree-approximated TDGL equation, given by,

$$i\gamma \frac{\partial}{\partial t} \psi(\mathbf{x}t) = \frac{1}{2m} (-i\nabla - q\mathbf{A}(\mathbf{x}t))^2 \psi(\mathbf{x}t) - \mu_{\text{pair}}(T) \psi(\mathbf{x}t) + D(\mathbf{x}t) \quad (4)$$

Here $\langle D^*(\mathbf{x}'t') D(\mathbf{x}t) \rangle = 2\gamma_2 T \delta(t - t') \delta(\mathbf{x} - \mathbf{x}')$, and $\gamma = \gamma_1 + i\gamma_2$. In order for Eq. (3) to be consistent with Eq. (4) we require that $\widetilde{\Sigma}_2(\omega) = 2\gamma_2 \omega$ and $\widetilde{\Sigma}_1(\omega) = \text{const.} + (1 -$

$\gamma_1)\omega$ at small ω . Similarly, we require that the pair chemical potential $\mu_{\text{pair}} \equiv \max_{\mathbf{k}} (\widetilde{T}(\mathbf{k}, 0)^{-1}) \propto (T - T_c)$ near T_c . The microscopic crossover picture[5, 13, 17] of BCS to BEC serves, via the small \mathbf{k} , ω dependence of $\widetilde{T}(\mathbf{k}, \omega)$, to constrain $\mu_{\text{pair}}(T)$, and complex γ . Here $|\mu_{\text{pair}}(T)|$ inversely varies with the number of bosons, and in the vicinity of T_c , is expected to be smaller than its BCS counterpart. It diverges at T^* where Bose degrees of freedom vanish. The lifetime of the bosons rapidly increases relative to BCS with increasing $(T^*/T_c - 1)$. The cuprates are believed to be in the fermionic regime, away from true BEC, where $|\gamma_1|/\gamma_2 \leq 1$.

The electric current \mathbf{J}^0 and heat current \mathbf{J}^1 follow from charge and energy conservation:

$$J_a^n(\mathbf{x}t) = \frac{q^{1-n}}{2V} \left\{ \left(i \frac{\partial}{\partial t} - q\varphi(\mathbf{x}t) \right)^n \psi(\mathbf{x}t) \right\}^\dagger \cdot \sum_{\mathbf{u}} iu^a \varepsilon_{\mathbf{ux}} \exp(-iqC_{\mathbf{ux}}(t)) \psi_{\mathbf{x}+\mathbf{u}}(t) + \text{h.c.} \quad (5)$$

When a small magnetic field $B_{ab} \equiv \frac{\partial}{\partial x_a} A_b - \frac{\partial}{\partial x_b} A_a$ is applied to the system, surface electric and heat currents appear in a thin shell around its boundary. This leads to

$$M_{ab}^n = \frac{q^{2-n}}{6} B_{cd} \int \frac{d^d k}{(2\pi)^d} \frac{d\omega}{2\pi} \Delta_{abcd} \text{Re} i \widetilde{T}(\mathbf{k}\omega)^2 \omega^n b(\omega), \quad (6)$$

where M_{ab}^0 is the usual magnetization, M_{ab}^1 is the thermal analogue[18] of M_{ab}^0 , $\Delta_{abcd}(\mathbf{k}) \equiv \frac{1}{2}(v_{ac}(\mathbf{k})v_{bd}(\mathbf{k}) - v_{ad}(\mathbf{k})v_{bc}(\mathbf{k}))$, and $v_{ab}(\mathbf{k}) \equiv \frac{\partial^2}{\partial k_a \partial k_b} \varepsilon(\mathbf{k})$ is the inverse mass tensor of the bosons, whose group velocity is given by $v_a(\mathbf{k}) \equiv \frac{\partial}{\partial k_a} \varepsilon(\mathbf{k})$.

For small, but constant B_{ab} , electric field $E_a^0 \equiv E_a$, and negative thermal gradient $E_a^1 \equiv -\frac{\partial}{\partial x_a} T$, the bulk volume current \mathbf{J}^n must be combined with surface contributions so that the net ‘‘transport’’ currents are given by:

$$J_{(\text{tr})a}^n = \langle J_a^n \rangle + \frac{\partial M_{ab}^n}{\partial T} E_b^1 + \delta_{n,1} M_{ab}^0 E_b^0. \quad (7)$$

The DC transport coefficients, defined by $J_{(\text{tr})a}^n = \sum_{n'=0}^1 \sum_b L_{ab}^{nn'} E_b^{n'}$, (which are readily related to α, σ) are

$$L_{ab}^{nn'} = \frac{q^{2-n-n'}}{2T^{n'}} \int \frac{d^d k}{(2\pi)^d} \frac{d\omega}{2\pi} v_a v_b \widetilde{A}^2 \omega^{n+n'} b^{(1)} + \frac{q^{3-n-n'}}{6T^{n'}} \int \frac{d^d k}{(2\pi)^d} \frac{d\omega}{2\pi} v_a v_c v_{bd} \widetilde{A}^3 \omega^{n+n'} b^{(1)}, \quad (8)$$

where $b^{(1)}(\omega) \equiv -\frac{\partial b(\omega)}{\partial \omega}$, $L_{ab}^{00} = \sigma_{ab}$ is the isothermal electric conductivity, L_{ab}^{11} is the isoelectropotential thermal conductivity, and $L_{ab}^{01} = \alpha_{ab}$ and L_{ab}^{10} are off-diagonal coefficients. Eq. (8) satisfies the Onsager relation[9] $T^{n'} L_{ab}^{nn'}(\vec{B}) = T^n L_{ba}^{n'n}(-\vec{B})$ (no summation), as a consequence of our inclusion of the surface terms[9]. Surface effects enter into L_{ab}^{01} , L_{ab}^{10} and L_{ab}^{11} , but cancel in L_{ab}^{00} .

Finally, we deduce the boson contribution to the complex ac conductivity and ac Hall conductivity

$$\begin{aligned}
\tilde{\sigma}_{ab}(\omega) &= \frac{iq^2}{\omega} \int \frac{d^d k'}{(2\pi)^d} \frac{d\omega'}{2\pi} v_a(\mathbf{k}') v_b(\mathbf{k}') \tilde{A}(\mathbf{k}'\omega') b(\omega') \\
&\cdot (\tilde{\mathcal{T}}(\mathbf{k}', \omega' + \omega) + \tilde{\mathcal{T}}^*(\mathbf{k}', \omega' - \omega) - \tilde{\mathcal{T}}(\mathbf{k}'\omega') - \tilde{\mathcal{T}}^*(\mathbf{k}'\omega')) \\
&+ \frac{iq^3}{2\omega} B_{cd} \int \frac{d^d k'}{(2\pi)^d} \frac{d\omega'}{2\pi} v_a(\mathbf{k}') v_c(\mathbf{k}') v_{bd}(\mathbf{k}') \tilde{A}(\mathbf{k}'\omega') b(\omega') \\
&\cdot (i\tilde{\mathcal{T}}(\mathbf{k}', \omega' + \omega) - i\tilde{\mathcal{T}}^*(\mathbf{k}', \omega' - \omega)) \\
&\cdot (\tilde{\mathcal{T}}(\mathbf{k}', \omega' + \omega) + \tilde{\mathcal{T}}^*(\mathbf{k}', \omega' - \omega) - \tilde{\mathcal{T}}(\mathbf{k}'\omega') - \tilde{\mathcal{T}}^*(\mathbf{k}'\omega')). \tag{9}
\end{aligned}$$

It can be verified that $\tilde{\sigma}_{ab}(\omega \rightarrow 0) = L_{ab}^{00}$ and that Eq. (9) satisfies the f-sum rule.

We illustrate the simple physics outlined above for a variety of normal state transport coefficients in which the bosonic contributions are dominant (over their fermionic counterparts). Here we consider one particular parameterization[19] of $\tilde{\Sigma}_2(\omega)$, although we have studied others as well. To facilitate the numerics we chose a simple formula for $\tilde{\Sigma}_2(\omega)$ that has both the linear dependence consistent with TDGL at small ω and vanishes at high frequencies: $\tilde{\Sigma}_2(\omega) = \frac{2\Omega_o p_2 \omega}{(\omega - p_1)^2 + p_2^2}$, where $p = p_1 + ip_2 = \frac{\Omega_o}{\gamma^* - 1}$, and Ω_o is the high frequency cut-off. More complex functional forms for $\tilde{\Sigma}_2(\omega)$ can be considered. Their primary effects are not so different from introducing new Ω_o , which does not alter the low frequency physics which we address here. We adopt a bandstructure $\tilde{\Sigma}_1(0) + \varepsilon(\mathbf{k}) = -\mu_{\text{pair}} + \mathcal{E}_1(1 - \cos(k_1 l_1)) + \mathcal{E}_1(1 - \cos(k_2 l_2)) + \mathcal{E}_3(1 - \cos(k_3 l_3))$. Measurements of the ac conductivity, discussed below provide a constraint also consistent with BCS-BEC physics: that the pair lifetime may be of the order of 100 times the BCS value for moderate underdoping ($T^*/T_c \approx 3$). We have systematically computed transport coefficients for the TDGL ratio γ_1/γ_2 ranging from about 0 to order unity. Provided we fit T^*/T_c to experiment, and presume the cut-off frequency Ω_o is a typical electronic scale, varying between 0.3eV and 3eV, the results presented here are robust to changes in the details of this parameterization, which is chosen to be consistent with BCS-BEC physics.

In Fig. 1 we plot the transverse thermoelectric coefficient α_{xy} vs T for three underdoped samples with indicated T^*/T_c . The arrows show the corresponding values of T_c which progressively decrease as T^*/T_c increases. The inset plots (unpublished) experimental data on $\text{La}_{2-x}\text{Sr}_x\text{CuO}_4$ from Ref. 20 which curves are for $x = 0.12, 0.07,$ and 0.03 and which are in rough correspondence to the values of T^*/T_c in the three theory plots. In both theory and experiment the dotted lines are for a non-superconductor $T_c = 0$. The onset temperatures are of the order of $T^*/2$, as in experiment. In the vicinity of T_c , the calculated behavior of α_{xy} corresponds to that of TDGL theory, albeit with modified coefficients.

Thus α_{xy} diverges at T_c although ν is finite there[9]. Similarly, with overdoping the behavior becomes characteristic of a more conventional fluctuation picture[9] in which $T^* \approx T_c$. The essential distinction between TDGL and the present case is that the onset temperature for bosonic contributions can be substantially higher than the conventional fluctuation regime. This figure illustrates the fact that α_{xy} (as well as ν) vanish at $T = 0$ in non-superconducting samples. This derives from the behavior of the Bose factor which has vanishing first derivative at $T = 0$. Semi-quantitative agreement between theory and experiment appears quite satisfactory.

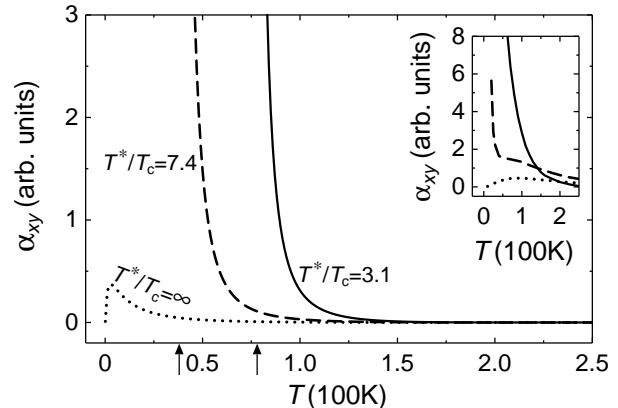


FIG. 1: Theoretical curves for the normal state α_{xy} with variable T^*/T_c ; experimental counterparts[20] in inset for $\text{La}_{2-x}\text{Sr}_x\text{CuO}_4$ at $x = 0.03, 0.07,$ and 0.12 .

An interesting inference from the data[2] is that, while, there is a considerable precursor effect for α_{xy} , the (orbital) magnetization drops to its superconducting value only in the immediate vicinity of Bose condensation. This quantity [given as M_{ab}^0 in Eq. (6)] is plotted in the inset to Fig. 2, for the same parameter set as in Fig. 1. The fermionic background (measured experimentally) is negligible, so that the bosonic contribution necessarily dominates. The sharpness of the Meissner onset (which clearly reflects T_c and not T^*) can be attributed to the small ratio of the boson velocity to the speed of light (and the small size of the hyperfine constant). Similar results hold in TDGL-based calculations.

In the main body of Fig. 2 are plotted the real and imaginary components of the ac conductivity as a function of T for $\omega \approx 100$ GHz for two different values of T^*/T_c , as in the previous figure. Both $\sigma_1 = \text{Re}\sigma$ and $\sigma_2 = \text{Im}\sigma$ are finite at T_c with σ_2 only slightly larger than σ_1 . The associated frequency dependence reflects the well known[7] $1/\sqrt{\omega}$ behavior of TDGL. It follows from TDGL that $d\sigma_1/dT$ is finite while $d\sigma_2/dT$ diverges at T_c . This latter prediction is the most notable difference between theory and experiment[3], although small sample inhomogeneities may smooth out a derivative divergence in the data. The theoretically deduced onset

temperature T_σ^* , for precursor effects in σ_2 can be estimated by noting that the fermionic background is relatively negligible so that σ_2 becomes appreciable when it reaches a few percent of its value at T_c . This corresponds to onset temperatures which are factors of 2 or so below those estimated from α_{xy} .

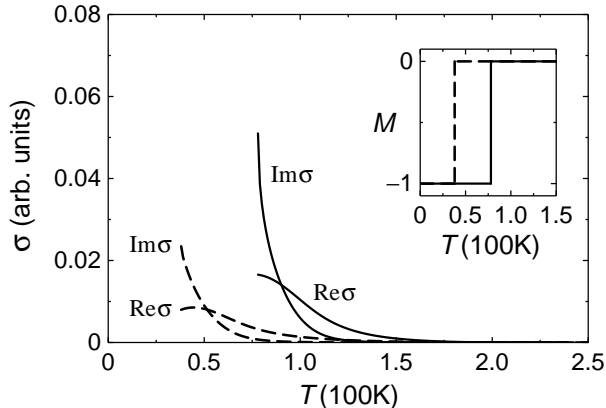


FIG. 2: Real and imaginary components of normal state σ at 100 GHz vs T . Solid and dashed curves have same T^*/T_c as for counterparts in Fig. 1. Associated magnetizations are plotted in inset, with the external magnetic field chosen as the unit.

Finally, in Fig. 3 we replot the calculated ac conductivity (for $T^*/T_c = 3.1$), following the Kosterlitz-Thouless (KT)-based analysis of Ref.3. In the main figure we illustrate these KT parameters (which are the basis of an interpretation of conductivity data in terms of vortices above T_c) via plots of $\phi \equiv \tan^{-1}(\sigma_2/\sigma_1)$ and $|S|$ as a function of ω/Ω obtained from $\sigma(\omega) \propto T_\theta^0(T)S(\omega/\Omega)\Omega^{-1}$. As in the data, here, T_θ^0 and Ω are deduced parameters. The inset plots $\tau = 1/\Omega$ as a function of temperature. We find that T_θ^0 is roughly constant in T , in contrast to the data which finds this quantity to be decreasing as T increases. Nevertheless, the agreement with experiment for all three quantities plotted in Fig. 3 is quite good. *In this way one might argue that key features of the ac conductivity data in Ref. 3 and attributed to KT physics, may equally well be explained by pre-formed pairs.*

Indeed, the reasonable agreement between the generic results of this theory and experiment for all three figures provides support for a preformed-pair alternative to the vortex scenario. Non-condensed bosons are also present below T_c and, thereby, will lead to some continuity between transport coefficients across the transition. In extending this work to the *ordered* phase, however, it will be useful to find a relationship between bosons and vortices. Along these lines is the dual representation explored earlier[21] in which vortices are the basic particles, rather than Cooper pairs.

Work supported by NSF-MRSEC Grant No.DMR-0213745. We thank Y. Wang and N. P. Ong for unpublished data, and G. Mazenko for useful conversations.

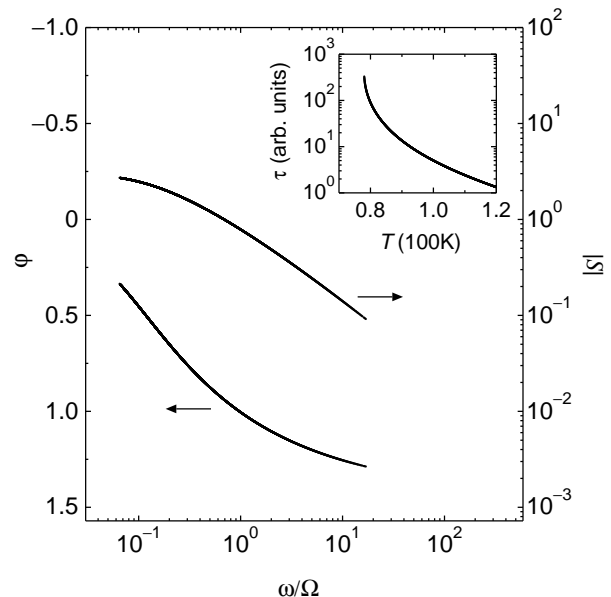


FIG. 3: Fits to Kosterlitz-Thouless (KT) scaling of the conductivity which can be compared to the analysis in Ref.3. See text for details.

-
- [1] Z. Xu, N. Ong, Y. Wang, T. Kakeshita and S. Uchida, Nature **406**, 486 (2000).
 - [2] Y. Wang, Z. A. Xu, T. Kakeshita, S. Uchida, S. Ono, Y. Ando and N. P. Ong, Phys. Rev. B **64**, 224519 (2001).
 - [3] J. Corson, R. Mallozzi, J. Orenstein, J. N. Eckstein and I. Bozovic, Nature **398**, 221 (1999).
 - [4] V. J. Emery and S. A. Kivelson, Nature **374**, 434 (1995).
 - [5] M. Randeria, in *Bose Einstein Condensation*, edited by A. Griffin, D. Snoke and S. Stringari (Cambridge Univ. Press, Cambridge, 1995), pp. 355-92.
 - [6] Q. J. Chen, I. Kosztin, B. Janko and K. Levin, Phys. Rev. Lett. **81**, 4708 (1998).
 - [7] A. Larkin and A. Varlamov (2001), cond-Mat/0109177.
 - [8] S. Ullah and A. T. Dorsey, Phys. Rev. B **44**, 262 (1991).
 - [9] I. Ussishkin, S. Sondhi and D. Huse, Phys. Rev. Lett. **89**, 287001 (2002).
 - [10] B. R. Patton, Phys. Rev. Lett. **27**, 1273 (1971).
 - [11] A. J. Leggett, in *Modern Trends in the Theory of Condensed Matter* (Springer-Verlag, Berlin, 1980), pp. 13-27.
 - [12] P. Nozières and S. Schmitt-Rink, J. Low Temp. Phys. **59**, 195 (1985).
 - [13] Jelena Stajic, A. Iyengar, Q. Chen and K. Levin, cond-mat/030615.
 - [14] A. Caldeira and A.J. Leggett, Physica **121A**, 587 (1983).
 - [15] Francisco Guinea, Phys. Rev. Lett. **53**, 1268 (1984)
 - [16] D.Z. Liu and K. Levin, Physica C **275**, 81-86 (1997)
 - [17] J. Maly, B. Janko and K. Levin, Physica C **321**, 113 (1999).
 - [18] In the present case there is no particle-hole symmetry and we consider T away from T_c so that the thermal surface magnetization is non-zero.
 - [19] For our underdoped samples, we chose $T_c = \max(0, T')$, where $T' = 1.6T^* - 0.5T^{*2} - 0.18$; with temperature

averaged quantities $\gamma_1 = 0.01 + 0.1(1 - T'/T^*)$, and $\gamma_2 = 5 + 10T'/T^*$; $\mathcal{E}_3/\mathcal{E}_1 = 10^{-4}$, and $-\mu_{\text{pair}} = \frac{(T^* - T')^2(T - T')^2}{(T^* - T)^2} + \frac{T'^2(T - T')}{T^{*2}}$. Here the unit of energy is

100K and $\mathcal{E}_1 = 15$, while $\Omega_o = 100$.

- [20] Yayu Wang and N. P. Ong, private communication.
 [21] M.A. Fisher and D.H. Lee, Phys. Rev. B **39**, 2756 (1989).